EURD OBSERVATIONS OF INTERSTELLAR RADIATION

JERRY EDELSTEIN, STUART BOWYER, ERIC J. KORPELA and MICHAEL LAMPTON
Space Sciences Laboratory, University of California, Berkeley, CA 94720-7450

JOAQUÍN TRAPERO*, JOSÉ F. GÓMEZ, CARMEN MORALES and VERONICA OROZCO
Laboratorio Astrofísica Espacial y Física Fundamental, INTA, Apdo. Correos 50727, E-28080 Madrid, Spain

Abstract. The hot interstellar medium (ISM) has far-reaching effect upon the structure of galaxies. Although ISM heating processes are fairly well understood, after decades of study, the processes that cool the hot interstellar medium remain obscure. The EURD spectrograph was designed to measure the diffuse cosmic background from 350 to 1100 Å in order to study the hot ISM and the mechanisms by which it sheds its energy. We present the first analysis of EURD observations of the cosmic background. These EURD observations have proven to be far more sensitive than previous work; compared to previous results, we have improved the limits to the intensity of 450 to 900 Å line emission from the ISM by one to two orders of magnitude. Our limit to OVI 1032 Å/ 1038 Å doublet of 7900 ph s^{-1} cm^{-2} str^{-1} is the lowest yet reported. The EURD limits to line emission are less intense than predicted by a variety theoretical models of the local ISM.

1. Introduction

The extreme ultraviolet (EUV) diffuse background is the most poorly known of any of the diffuse astronomical backgrounds. Because of the observational complexity of background measurements in the EUV bandpass, only upper limits to this flux exist. The limits have been obtained with spectrometers with very crude (from ≈ 15 to 30 Å) resolution (Holberg, 1986; Labov and Bowyer, 1991) and are generally one to two orders of magnitude larger than the expected sources of cosmic flux. A variety of source mechanisms have been postulated to radiate in this bandpass; the most discussed is the poorly understood hot gas in the interstellar medium. The actual lines observed from a hot ISM will be strongly dependent upon the temperature and thermal history of this material (Breitschwerdt and Schmutzler, 1994). Several temperatures have been suggested for this phase. Soft X-ray data suggest 10^6 K gas (Cox and Reynolds, 1987). Absorption line data showing O VI (Jenkins, 1978a,b) is often cited in combination with the soft X-ray data as further evidence for a 10^6 K gas, but the peak of the emission curve for O VI is at the substantially lower temperature of $\sim 3 \times 10^5$ K. High ionization absorption lines

* Present address: Universidad SEK, Cardenal Zúñiga s/n, Segovia, Spain

Astrophysics and Space Science is the original source of this article. Please cite this article as: *Astrophysics and Space Science* **276:** 177–185, 2001.

observed in stellar spectra taken with *IUE* indicate a temperature of 3×10^5 K (Savage, 1987) as does the observation of emission lines at far UV wavelengths (Martin and Bowyer, 1989). Breitschwerdt and Schmutzler (1994) have suggested that the soft X-ray emission is the product of residual high ionization states and that the actual kinetic temperature of this plasma could be as low as 4×10^4 K.

In this paper we report results of spectral observations made with in the 350–1100 Å region, where the radiation from cooling local plasmas is predicted to occur, and compare the results obtained with the expected flux.

2. Observations

From the past two years, on the MINISAT 01 spacecraft, the Espectrógrafo Ultravioleta extremo para la Radiación Difusa (EURD) has been conducting sensitive measurements of the diffuse UV background. Two spectrographs cover the 350–1100 Å region with a spectral resolution of $\sim$ 6 Å (Bowyer *et al.*, 1997). The Long Spectrograph measures 550–1100 Å and the Short Spectrograph measures 350–900 Å. The data analyzed were selected from the first 6 months of the mission, between July 1998 and December 1998.

EURD data are taken via a continuous sequence of aperture exposures: Open, Closed, and a MgF_2 filter. The Open position provides spectral data plus backgrounds. The MgF_2 filter position gives an estimate of the instrumental scattering of geocoronal Ly α radiation. The Closed position gives an estimate of the internal background. The exposures periods for the Open, Closed and MgF_2 apertures are 30, 45, and 15 seconds, respectively. Each photon carries information regarding the event's detector pulse-heigth and an anti-coincidence flag which indicates an event-simultaneous triggering of the anti-coincidence shield surrounding the detector. Internal background components include energetic charged particles and their interaction products that are missed by the anti-coincidence system, and radioactivity within the detector and in the spacecraft.

Data are quality selected to insure accurate counting rate determination and to minimize background sources, and then processed to remove detector distortions. Exposures are examined and rejected (3% of the data) in the case of telemetry loss. Events near the detector's distorted-image edge are rejected. Individual events are filtered for acceptable detector pulse-height and anti-coincidence rejected ($\sim$ 20% of the data). The data contain artificial stimulation events which mark fixed detector locations. In order to correct for image shifts due to electronic instabilities, the detector image for each exposure is shifted according the centroid of the stimulation events. Typical shifts correspond to a few Å in the spectral dimension. Detector image distortion was corrected using a polynomial warping procedure. The distortion matrix was derived from a combination of ground calibration data and observations of spectral line locations from Moon observations.

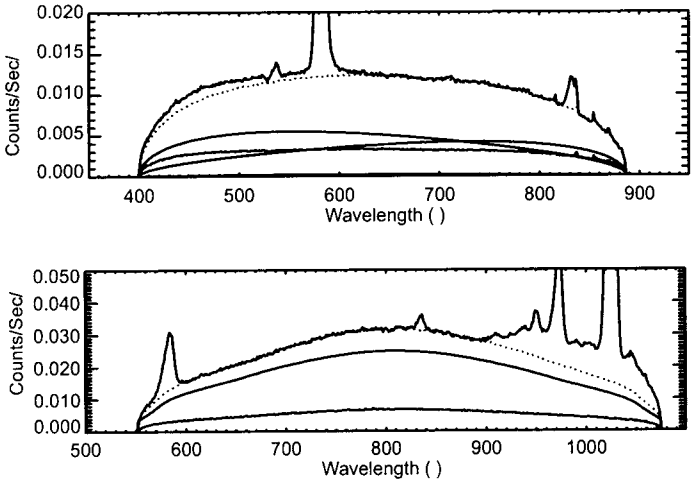

Figure 1. EURD data and background components for the Short (upper panel) and Long (lower panel) spectrographs. The Open aperture spectrum is the upper, solid data line. The MgF_2 aperture spectrum is the lower, solid data line. The smooth lines show modeled out-of-band airglow contributions. The Closed aperture spectrum is indistinguishable from the 'X' axis.

Higher count rates are always experienced at spacecraft sunrise and sunset due to geocoronal effects, but deep night intensities are typically constant and low. For the search for faint cosmic radiation, we selected for data taken with solar zenith angles greater than 150 degrees and eliminated data associated with anomalously high backgrounds rates between 850 to 900 Å. We eliminated data containing FUV bright stars for Long spectrograph data with $\lambda > 900$ Å by testing for anomalous levels of flux between airglow lines. The viability of the star-test was checked by confirmation of the existence of the directly imaged stellar spectrum for bright objects. Observations including the Moon also were deleted from the data set.

The resulting dark-night data for each aperture of the Long and Short Spectrographs are shown in Figure 1. The Short wavelength band used 1.2×10^6 seconds of 'open' data containing 7.5×10^6 events. The Long wavelength band using 3×10^5 seconds of 'open' data containing 4.7×10^6 events. The Open aperture data clearly shows airglow lines residing upon a background. We attribute the background to grating scattered photons arising from the wings of the zero and first order of geocoronal hydrogen and helium Ly α whose peaks were designed to fall beyond the ends of the detector. The MgF_2 aperture directly measures the hydrogen Ly α scattering. We have included modeled scattering for the geocoronal radiation not measured with the MgF_2 aperture.

The net EURD spectra, derived by using a flux conversion factor, are shown in Figure 2 along with the 2σ statistical counting errors due to the signal and background components. The data from the Long and Short spectrographs were combined in their region of overlap from 600 to 900 Å. The high frequency features longward of 850 Å are detector artifacts. We determined the EURD counts-to-

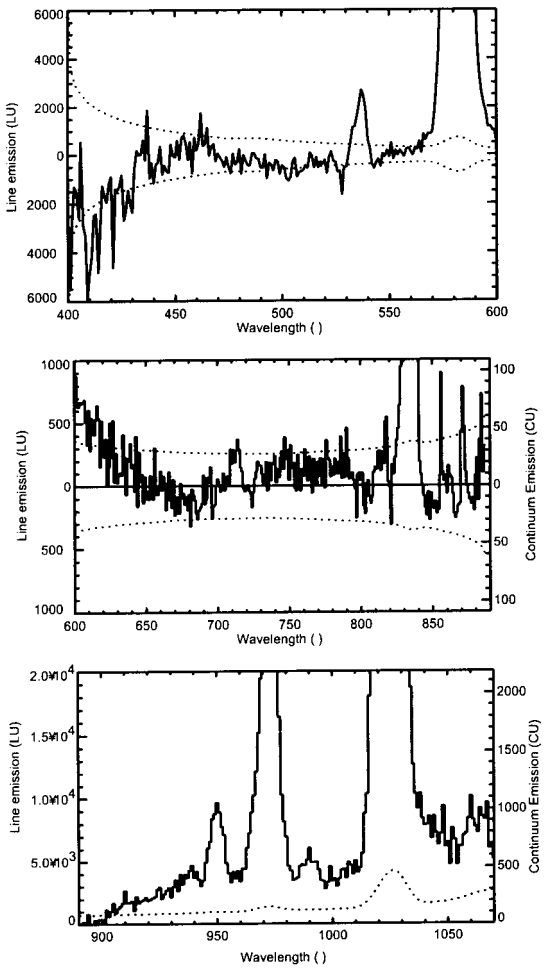

Figure 2. The Net EURD spectra (solid line) are shown for three sub-bands in the three panels. Statistical counting errors (2σ) are shown by the dashed line. Corresponding scales for limits to single line emission and continuum emission are shown.

flux conversion factor using an in-flight calibration strategy based on simultaneous EUV observations of the Moon with EUVE and EURD (Flynn *et al.*, 1998), and, longward of 912 Å, to fits to stellar spectra (Morales *et al.*, 1999; *Astrophys J.*, submitted). It is estimated that this calibration is good to $\pm 20\%$ in the band around 912 Å. The geocoronal helium Ly α and Ly β are clearly visible, along with geocoronal hydrogen series from Ly β shortward. Also visible are the OI 834 Å and 989 Å lines, as well as the faint O 911 Å recombination feature. An unknown feature is suggested at about 710 Å. The counting errors correspond to the upper limits for single line emission and, by using the 9.1 Å effective width of the spectral profile, to upper limits for continuum.

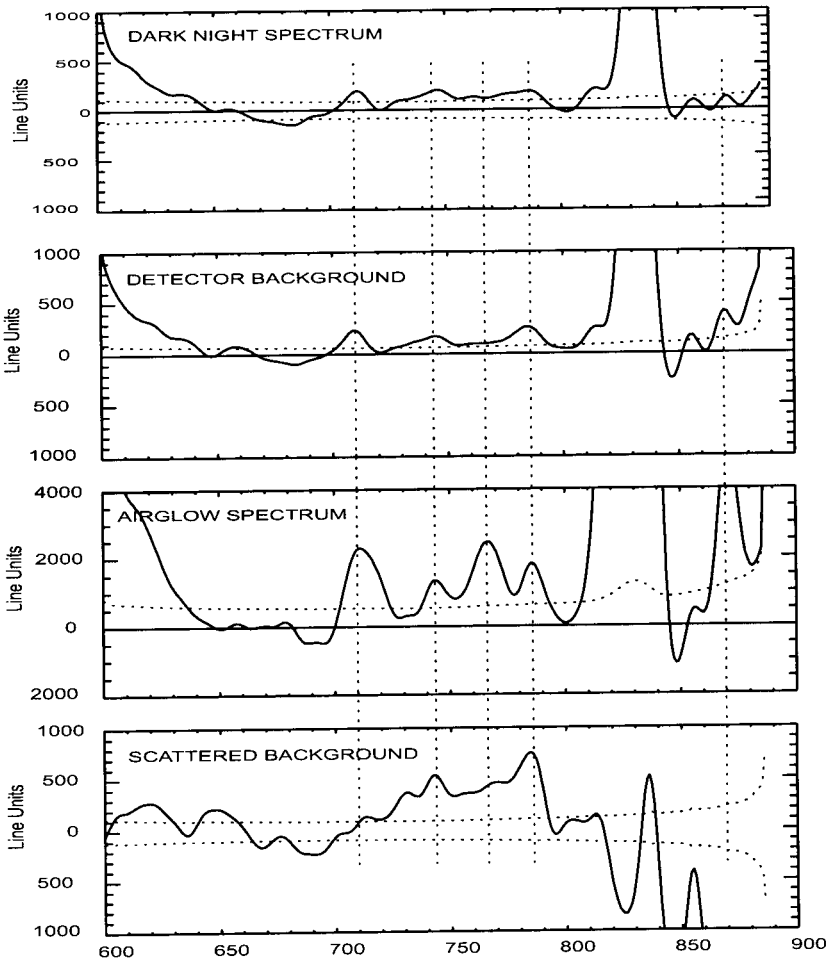

Figure 3. The combined Long and Short spectra, after smoothing with the spectral line profile, for the different apertures and for an airglow-bright period. Dotted lines aid the comparison of features in the spectra.

We examined the possible origins of features in the 600 to 900 Å bandpass by comparing our dark-night spectra (Open aperture) with the spectra from the detector background (Closed aperture), the spectra of the scattered background (MgF_2 aperture) and spectra from periods with bright airglow (Open aperture). We compare these spectra, smoothed by the line spread function, in Figure 3. Certain features such as those at 742 Å and 783 Å appear in all cases. Other features such as the one at 710 Å and 763 Å and 870 Å are certainly enhanced in the airglow spectrum. We attribute the features that are persistent in the airglow and detector-background spectrum to modulations in the flat-field response of the micro-channel

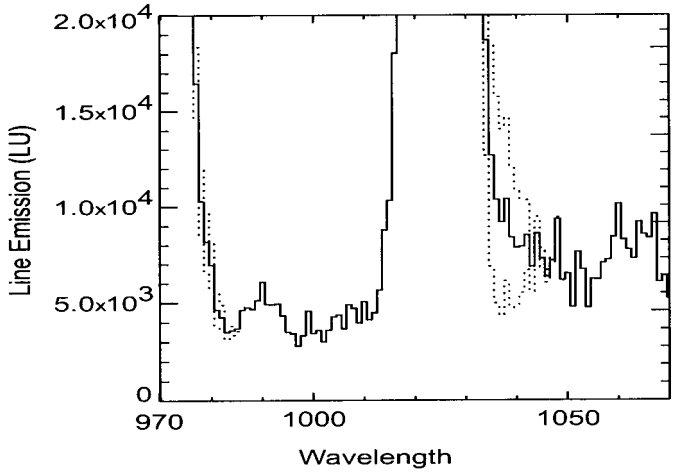

Figure 4. The Long Spectrograph Net spectra is shown (solid line) along with the 3σ statistical deviation (dashed line) attibutable to 7900 ph s^{-1} cm^{-2} str^{-1} of OVI and 1900 ph s^{-1} cm^{-2} str^{-1} of CIV emission.

plate detector. Consequently, we are not prepared to claim that any feature is a definitive detection of cosmic background flux.

To examine for the presence of the specific features OVI 1032 + 1038 Å and CIII 977 Å in the presence of the bright hydrogen airglow lines at 1026 Å and 972 Å, we calculated the Long Spectrograph net spectra that would be result from a 3σ statistical deviations at those wavelengths. The resultant spectrum is shown in Figure 4 along with the original net-spectrum. By inspection, our 3σ limit of 7900 ph s^{-1} cm^{-2} str^{-1} to OVI combined doublet emission seem quite secure because of the adequate separation of the 1038 Å feature from the airglow line. On the other hand, the 3σ limit of 1900 ph s^{-1} cm^{-2} str^{-1} to CIII is less secure because the EURD spectral resolution does not well separate this feature from the airglow.

3. Discussion and Conclusions

The EURD 2σ upper limits to single line emission are shown in Figure 5 in comparison with previous observations and theoretical predictions. In the 450–900 Å bandpass, our limits to line emission represent a one to two order of magnitude improvement in comparison to previous results (Holberg, 1986; Labov and Bowyer, 1991; Edelstein *et al.*, 1999). Furthermore, the EURD limits have been obtained with at least a factor of five improvement in spectral resolution, for a robust treatment of background components.

The EURD data from 500–700 Å appear to be completely incompatible with models of emission from hot steady-state 10^6 K equilibrium plasma found to be

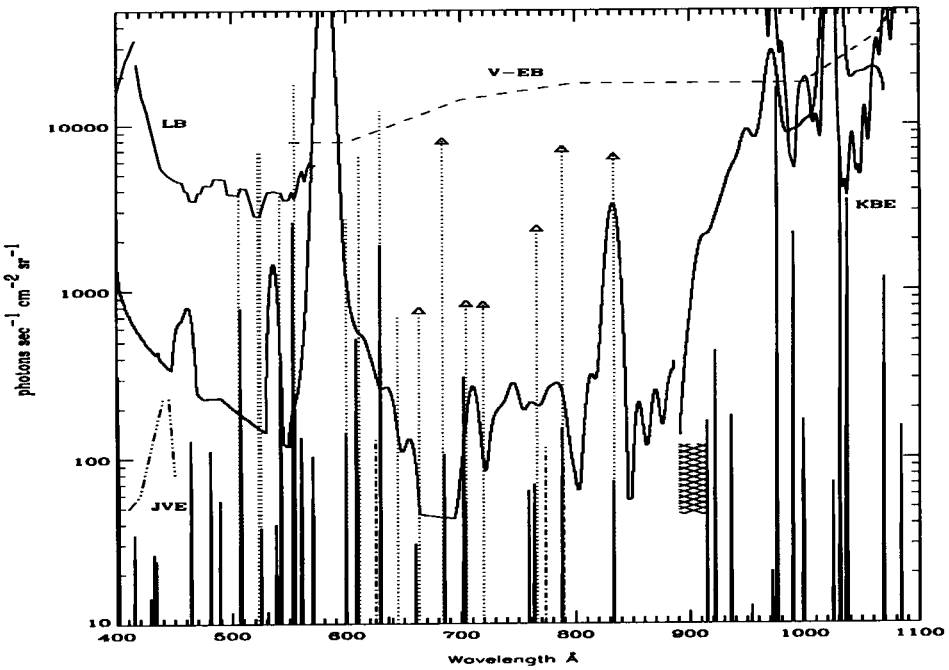

Figure 5. EURD Limits to the diffuse EUV cosmic background are shown by the thick curved line. The limits are 2σ bounds to single line emission. Existing upper limits are shown; LB is the 15A resolution upper limit of Labov (1991). V-EB is the 30A resolution upper limit derived from Voyager (Edelstein *et al.*, 1999). JVE are the upper limits of Jelinsky *et al.* (1995). Theoretical predictions are shown; The thin dotted vertical lines capped with triangles are preliminary predicted intensities from the delayed recombination model of Breitschwerdt and Schmutzler (1999). The thin solid vertical lines are the expected ISM emission from a steady-state 10^6 K equilibrium plasma consistent with X-ray measurements (Bloch, 1986). The thick solid vertical lines are emission expected from a supernova bubble of Slavin and Cox (1993). The thick dashed vertical lines are emission expected from the local bubble's conductive interface (Slavin, 1989). The cross-hatched region shows the range of the emission signature predicted by Sciama (1994) for a Galactic halo of radiatively decaying neutrinos.

consistent with X-ray measurements (Bloch *et al.*, 1986) and with preliminary models of delayed recombination emission in this bandpass (Breitschwerdt, 2001, in this volume). Our data are also inconsistent with models of emission from the local bubble's evaporative cloud interface (Slavin, 1989) and with gas characteristic of the supernova bubble models of Slavin and Cox (1993).

Our upper limit to emission of the OVI doublet, 7,900 ph s^{-1} cm^{-2} str^{-1} are the lowest yet reported and are lower than the 4σ confidence $\sim$ 10,000 ph s^{-1} cm^{-2} str^{-1} detections of Dixon (1996). The EURD limit can be used to tighten constraints upon models of hot gas in the galactic corona (see Korpela *et al.*, 1998).

These EURD data also measure continuum background emission within the 900–1100 Å region, as shown in Figure 2. EURD's spectral resolution allows for careful measurements of the continuum between airglow features, unlike pre-

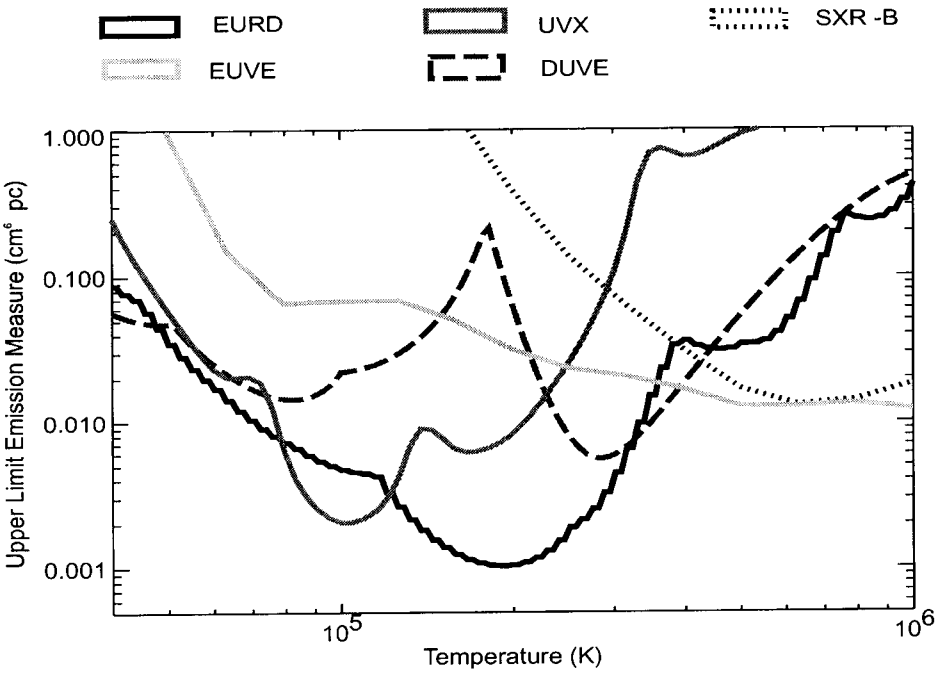

Figure 6. EURD 2σ upper limits to equilibrium plasma emission measure are shown by the thick dark curve. Local plasma of intermediate temperature is strongly excluded. Limits from previous measurements are shown; Limits from EUVE are shown by the light grey line (Jelinsky *et al.*, 1995). Limits from soft X-ray measurements (Bloch *et al.*, 1986), 1500–1800 Å measurements (UVX: Martin *et al.*, 1986), and 980–1080 Å measurements (DUV: Korpela *et al.*, 1998), are shown by the dotted, dark-grey, and dashed lines, respectively.

vious work (Murthy *et al.*, 1999). The EURD limits to continuum emission are 200 ± 80 ph s^{-1} cm^{-2} str^{-1} Å^{-1} at 920 Å and 350 ± 100 ph s^{-1} cm^{-2} str^{-1} Å^{-1} at 1000 Å. The value at 920 Å may be considered an upper limit because flux from the higher Lyman series components of geocoronal hydrogen emission lines is included. Establishing continuum values at $\lambda < 900$ Å is uncertain because of our background modeling procedure.

We have established new upper-limits to the emission measure of local thin plasma in thermodynamic equilibrium by comparing our emission line-limit results with theoretical predictions of plasma emission (Dere, 1997). Our limits to plasma emission measure are shown in Figure 6 in comparison with limits from previous measurements. The lowest emission measure limit of 0.001 cm^{-}6pc occurs at 125 000 K, thus strongly excluding local plasma of intermediate temperature. In comparison to *EUVE* limits to emission measure, the only other established limits which apply specifically to the local ISM, the EURD results have markedly improved the limits for temperatures below 170 000 K.

Acknowledgements

Funding for the instrument was provided by NASA grant NGR 05-003-450 and INTA grant IGE 490056. The UCB analysis and interpretation is carried out through the volunteer efforts of S. Bowyer, J. Cobb, J. Edelstein, E. Korpela and M. Lampton. The work by C. Morales, J. Trapero and V. Orozco is supported in part by DGCYT grant PB94-0007. J.F. Gómez is supported in part by DGYCIT grant PB95-0066 and Junta de Andalucía (Spain).

References

Bloch, J.J., Jahoda, K., Juda, M., McCammon, D., Sanders, W.T. and Snowden, S.L.: 1986, *Astrophys. J.* **308**, L59.
Bowyer, S., Edelstein, J. and Lampton, M.: 1997, *Astrophys. J.* **485**, 52.
Bowyer, S., Lampton, M., Peltoniemi, J. and Roos, M.: 1995, *Phys. Rev. D* **B25**, 3214.
Breitschwerdt, D. and Schmutzler, T.: 1994, *Nature* **371**, 774.
Breitschwerdt, D. and Schmutzler, T.: 1999, *Astron. Astrophys.* **347**, 650.
Breitschwerdt, D.: 2001, this volume.
Chakrabarti, S., Paresce, F., Bowyer, S. and Kimble, R.: 1983, *J. Gen. Relativ.* **88**, 4898.
Cox, D.P. and Reynolds, R.J.: 1987, *Annu. Rev. Astron. Astrophys.* **25**, 303.
Dixon, W.V.D., Davidsen, A.F. and Ferguson, H.C.: 1996, *Astrophys. J.* **465**, 288.
Dere, K.P., Landi, E., Mason, H.E., Monsignori Fossi, B.C. and Young, P.R.: 1997, *Astron. Astrophys. Suppl.* **125**, 149.
Edelstein, J., Lampton, M. and Bowyer, S.: 1999, *Astrophys. J.*, submitted.
Feldman, P., Davidson, A., Blair, W., Bowers, C., Durrance, S., Kriss, G., Ferguson, H., Kimble, R. and Long, K.: 1992, *Geophys. Res. Lett.* **19**, 453.
Flynn, B.C., Vallerga, J.V., Gladstone, G.R. and Edelstein, J.: 1998, *Geophys. Res. Lett.* **25**, 3253.
Holberg, J.B.: 1986, *Astrophys. J.* **311**, 969.
Jelinsky, P., Vallerga, J.V. and Edelstein, J.: 1995, *Astrophys. J.* **442**, 653.
Jenkins, E.B.: 1978a, *Astrophys. J.* **219**, 845.
Jenkins, E.B.: 1978b, *Astrophys. J.* **220**, 107.
Korpela, E.J., Bowyer, S. and Edelstein, J.: 1998, *495*, 317.
Labov, S.E. and Bowyer, S.: 1991, *Astrophys. J.* **371**, 810.
López-Moreno, J.J., Morales, C., Gómez, J.F., Trapero, J., Bowyer, S., Edelstein, J., Lampton, M. and Korpela, E.: 1998, *Geophys. Res. Lett.* **25**, 2937.
Martin, C. and Bowyer, S.: 1989, *Astrophys. J.* **338**, 677.
Morales, C.: 1999, *Astrophys. J.*, submitted.
Murthy, J., Hall, D., Earl, M. and Henry, R.C.: 1999, *Astrophys. J.*, in press.
Sciama, D.W.: 1994, *Modern Cosmology and the Dark Matter Problem*, Cambridge University Press, New York.
Slavin, J.D.: 1989, *Astrophys. J.* **346**, 718.
Slavin, J.D. and Cox, D.P.: 1993, *Astrophys. J.* **417**, 187.